RFX-mod2: a reversed-field pinch device with edge transport optimization

M. Veranda[1], P. Scarin[1], M. Agostini[1], D. Bonfiglio[1], S. Cappello[1], G. Spizzo[1], P. Zanca[1]

[1] *Consorzio RFX (CNR, ENEA, INFN,Università degli Studi di Padova, Acciaierie Venete SpA), Padova, Italy*

Introduction. The edge of magnetically confined hot plasmas in toroidal configurations is characterized by the presence of magnetic fluctuations with helicity *m/n*, with *m* and *n* the poloidal and toroidal mode numbers. In the reversed-field pinch device RFX-mod an almost-monochromatic spectrum develops in the whole plasma volume: this is the so-called quasi-single helicity plasma (QSH), characterized by enhanced confinement properties [1]. Edge measurements indicate the presence of a dominant mode with $m/n = 1/7$ and of a spectrum of nonlinearly interacting secondary modes [2], resulting in the possibility of constructive interference: a localized toroidal deformation of the edge radial magnetic field may thus be present where the modes are *phase locked*, with a position changing in time. Such localized deformation has negative effects on plasma-wall interaction (PWI) and on operations at high current.

The aim of this paper is to analyze the global PWI in QSH plasmas, both experimentally and numerically, for the RFX-mod and the upgraded RFX-mod2 device, soon starting operation [3]. This paper begins with the experimental characterization of the secondary modes locking in RFX-mod, and of its effect on PWI. Then, the features of the edge magnetic field topology will be described, together with a MHD description of secondary modes locking. Eventually, the positive effect of secondary modes mitigation expected in RFX-mod2 will be discussed.

The local radial magnetic deformation Δ (a.k.a. *shift*) of a given m/n mode is related to its perturbed radial field $b_{r,m/n}$ through [4]:

$$\Delta_{m/n}(t,\theta,\phi) = \frac{-iab_{r,m/n}(t,a)e^{i(m\theta-n\phi+\phi_{m/n}(t,a))}}{(m-nq(t,a))B_{0\theta}(t,a)}. \quad (1)$$

This formula is written considering a cylindrical geometry (r,θ,ϕ). $q(a)$ is the safety factor at the plasma edge a and $B_{0\theta}$ is the equilibrium poloidal field. The *m=1 secondary modes shift* is defined as $\Delta_{sec} = \sum_{n=8}^{n=23} \Delta_{1/n}$+c.c., and the dominant mode shift as $\Delta_{1/7}$. Another useful parameter is the ratio $S_k(t) = \max_{\theta,\phi}(\Delta_{sec}(t,\theta,\phi))/\max_{\theta,\phi}(\Delta_{1/7(t,\theta,\phi)})$: it measures the disturbance of the helix associated with the dominant mode caused by secondary perturbations. Such parameters, when evaluated at the edge $r = a$, contain a 2D information about plasma edge.

Experimental findings. Thanks to a full coverage of edge diagnostics along the poloidal and toroidal angles, it is possible to reveal the 3D structure of the PWI and to correlate its topology with the magnetic deformation due to the dominant $\Delta_{1/7}$ and secondary modes Δ_{sec}. All

the measurements indicate that an interferential pattern created by secondary modes causes a toroidally localized deformation Δ_{sec}, whose toroidal position changes in time.

Fig.1i shows the effect of the presence of a phase locking on PWI, considering two different frames taken from a CCD camera looking at the CI line at 970nm: panel a) shows the situation away from the localized toroidal deformation, while panel c) exhibits strong local emission of CI, in particular two "stripes" toroidally localized. The strong local emission of panel c) is well correlated with the two peaks of Δ_{sec} observed in panel d) around $\phi \sim 0$, while the smooth CI emission observed in panel a) is the due to the fact that phase locking, at this time, is located at 100°, outside the CCD camera field of view (see panel b). In Fig.1ii the temporal behaviour of the maximum Δ_{sec} and $\Delta_{1/7}$ (black and red lines in panel a) is shown: the shaded regions correspond to an increase of wall emission, which is well correlated with the condition $S_k \gtrsim 1$. Further experimental evidences are shown in [7] and describe the PWI shape as given by a helix rotating at few tens of Hz, distorted poloidally and with a localized toroidal deformation. In the next paragraph the effect of such deformation on the magnetic topology is described.

Connection length structures are evaluated computing the average length travelled by a bundle of 1000 magnetic field lines from an initial condition in the plane $(r,0,\phi)$ to the wall, namely L_{cw}. The calculation is performed with the ORBIT code, considering modes with $m = 0,1$ and $n = 1:24$ coming from the solution of ideal MHD Newcomb's equation [9]. The reference shot used is #37537, $I_P \sim 1.5$MA, $t = 130$ms where $S_k = 0.51$. The results are shown in Fig.2i. The toroidal shape of $L_{cw}(\phi)$ (panel a) reproduces the $n = 7$ dominant mode topology, but with a strong decrease in the region around $\phi = 120°$, corresponding to the region where two maxima of Δ_{sec} are observed (panel b). The two minima of L_{cw} in the locking region ($L_{cw,hole}$, shaded region in Fig.2i) can be associated quite well to the couple of stripes shown by the visible camera in Fig.1i: a similar phenomenon is observed in the X-point region of tokamaks when RMPs are applied and it is described as "homoclinic lobes" [5]. To assess the role of secondary perturbations on the edge topology, a scan of S_k is done by rescaling the amplitude of secondary modes fixing their phase and the dominant mode. The most interesting observation is an order-of-magnitude increase of L_{cw} when $S_k \lesssim 0.3$, i.e. decreasing secondary modes of about a factor of 2 (the same decrease foreseen in RFX-mod2, see the final remarks). One also notices a more regular behaviour of the mean value of connection length in the locking region $L_{cw,hole}$.

3D nonlinear viscoresistive MHD modelling gives a description of mode locking similar to the one coming from the experimental measurements previously described. With respect to the MHD simulation described in [7], more realistic boundary conditions take into account a thin resistive wall with resistive diffusion time τ_W at $r = a$, and a vacuum region surrounded

by an ideal wall at $r = b$, as described in [6]. A simulation with inversed normalized resistivity $S = 10^6$, inverse normalized viscosity $M = 10^4 >$, $b/a = 1.2$, $\tau_W/\tau_A = 10^4$ is analyzed. In panel a) of Fig.2ii a part of the temporal dynamics of the dominant $m = 1, n = 7$ MHD mode and of $m = 1$ secondaries is shown (the complete simulation can be found in [6]). During this snapshot a QSH states with $n = 7$ spontaneously appear , interrupted by relaxation events at around $t \sim 0.148\tau_R$ and $t \sim 0.154\tau_R$. We evaluate S_k (in panel b) and the shifts $\Delta_{1/7}, \Delta_{sec}$ at $r = a$ using $a = 0.459$m and $I_P = 1.5$MA to normalize the magnetic field. Despite the presence of a weak QSH state (red mark in panel b)) an interference pattern due to secondary modes is present at $\phi \sim 180^\circ$ (panel d). Panel c) instead shows a case with higher secondary shift, corresponding to the first relaxation event. A more quantitative agreement with respect to mean S_k values between numerical simulations and experiments could be achieved by performing simulations at a higher and more realistic value of inverse resistivity (in high current experiments at RFX-mod it is estimated $S \propto T^{3/2} \sim 5 \cdot 10^7$). Higher S produces a general decrease of secondary modes' intensity, and thus a reduction of S_k to values similar to the ones in Fig.1ii. Another case from MHD simulations with ideal magnetic boundary conditions is described in [7].

Considerations about RFX-mod2, and final remarks. The major upgrade foreseen on the RFX-mod machine is the removal of the vacuum vessel facing the plasma. As a result, the distance of the plasma from the stabilizing shell will be reduced, decreasing the intensity of secondary modes [8]. A twofold decrease of the magnetic deformation at the edge is expected. As a preliminary assessment of the resulting topology, the RFXlocking code [9] has been applied in two cases mimicking the two different front-end layouts (more details in [7]). The main prediction from the topological analysis is that the decrease of the plasma deformation should allow a clear increase of the connection length to the wall and the disappearance of the residual "hole" in the locking region , a feature expected to mitigate PWI. This opens the possibility of an edge transport in principle only affected by error fields at the gaps.

References

[1] R. Lorenzini *et al*, Nature Physics **5**, 570 (2009)

[2] G. Spizzo *et al*, Nucl. Fusion **57**, 126055 (2017)

[3] S. Peruzzo *et al*, Fus. Eng. Design **123**, 59 (2017)

[4] P. Zanca *et al*, Plasma Phys. Control. Fusion **46**, 1115 (2004)

[5] A. Punjabi, A. Boozer, Phys. Lett. A **378**, 2410 (2014)

[6] D. Bonfiglio *et al*, P1.1049 this Conference

[7] P. Scarin *et al*, Nucl. Fusion **accepted**, https://iopscience.iop.org/article/10.1088/1741-4326/ab2071 (2019)

[8] L. Marrelli, R. Cavazzana *et al*, Nucl. Fusion **59**, 076027 (2019)

[9] P. Zanca, Plasma Phys. Control. Fusion **51**, 015006 (2009)

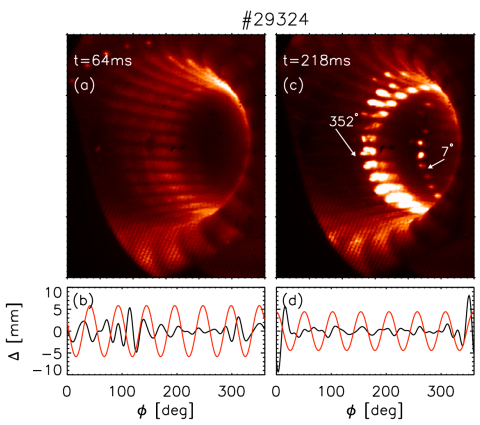

(i) Two CCD time frames during QSH states, with a field of view centered at $\phi = 0°$: in panel a) without presence of phase locking in the field of view and panel (c) with the locking. The corresponding toroidal amplitude of $\Delta_{1/7}$ (red line) and Δ_{sec} (black line) are shown respectively in panels b) and d)

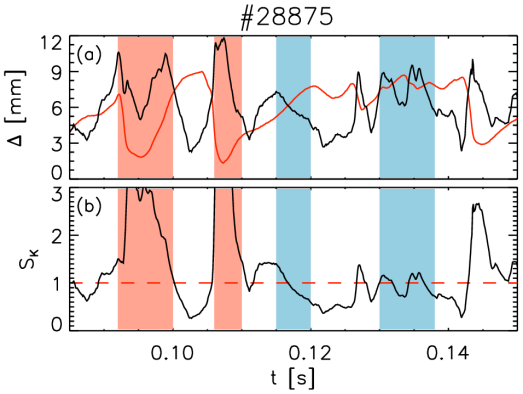

(ii) Time behavior of the maximum of interferential pattern in panel a). $\max_{\theta,\phi}(\Delta_{sec})$ (black line) compared with $\max_{\theta,\phi}(\Delta_{1/7})$ (red line); their ratio $S_k(t)$ is shown in panel b). Blue shaded areas correspond to time windows with increased wall emission in QSH state ($S_k > 0.7$), while red shaded area correspond to MH states.

Figure 1: Experimental results.

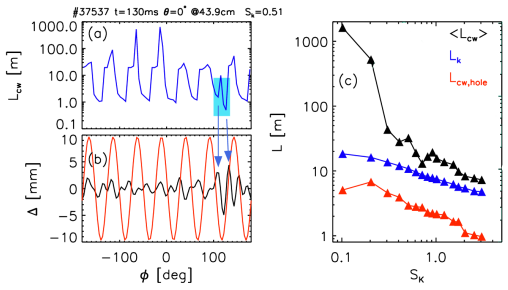

(i) Toroidal behavior of the connection length to the wall L_{cw}, simulation on the equatorial plane ($\theta = 0°$) with $S_k \sim 0.50$. Panel (b) behavior of $\Delta_{1/7}$ (red) and of Δ_{sec}. Panel (c) Scaling of L_{cw} simulation with S_k: the black line is the average value along the toroidal direction, the red line is the value in the locking region, the blue line is the Kolmogorov length. $\langle L_{cw} \rangle$ presents a threshold-like behavior at $S_k \sim 0.3$.

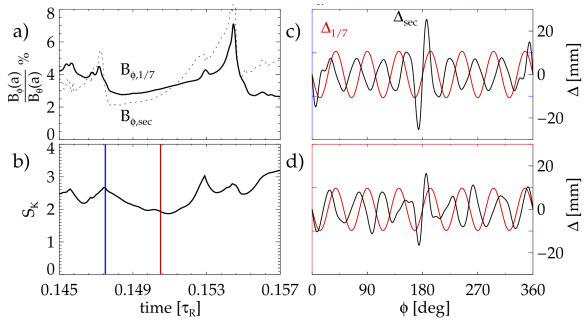

(ii) Evolution of a 3D nonlinear simulation of the RFP configuration (better described in [6]); a) single MHD cycle: the growth of dominant mode is disturbed by relaxation events; (b) time evolution of S_k during the MHD cycle, two different snapshots are identified (vertical lines); panels (c) and (d) toroidal behavior of the displacements Δ, corresponding to the two snapshots of panel (b) with $S_k > 2$ and $S_k < 2$.

Figure 2: Numerical results.